

Dynamics of social contagions with heterogeneous adoption thresholds: Crossover phenomena in phase transition

Wei Wang,^{1,2} Ming Tang,^{1,2,*} Panpan Shu,^{1,2} and Zhen Wang^{3,†}

¹Web Sciences Center, University of Electronic Science and Technology of China, Chengdu 610054, China

²Big data research center, University of Electronic Science and Technology of China, Chengdu 610054, China

³Interdisciplinary Graduate School of Engineering Sciences,
Kyushu University, Kasuga-koen, Kasugashi, Fukuoka 816-8580, Japan

Heterogeneous adoption thresholds exist widely in social contagions, but were always neglected in previous studies. We first propose a non-Markovian spreading threshold model with general adoption threshold distribution. In order to understand the effects of heterogeneous adoption thresholds quantitatively, an edge-based compartmental theory is developed for the proposed model. We use a binary spreading threshold model as a specific example, in which some individuals have a low adoption threshold (i.e., activists) while the remaining ones hold a relatively high adoption threshold (i.e., bigots), to demonstrate that heterogeneous adoption thresholds markedly affect the final adoption size and phase transition. Interestingly, the first-order, second-order and hybrid phase transitions can be found in the system. More importantly, there are two different kinds of crossover phenomena in phase transition for distinct values of bigots' adoption threshold: a change from first-order or hybrid phase transition to the second-order phase transition. The theoretical predictions based on the suggested theory agree very well with the results of numerical simulations.

PACS numbers: 89.75.Hc, 87.19.X-, 87.23.Ge

I. INTRODUCTION

Social contagions are ubiquitous in human society, and generate new scientific challenges for network science [1, 2]. All the researches about sentiments contagion, information spreading and behavior spreading fall into the category of studying social contagions [3, 4]. In particular, behavior spreading, as a representative and essential type of social contagions, has attracted great attention, both theoretically and experimentally [5, 6]. Understanding the spreading mechanisms behind behavior has the potential to not only help us design better anti-virus strategies [7], but also shed new insights into the control of social unrest [1]. Moreover, different from biological contagions (such as epidemic spreading) [8–13], social contagions display one inherent characteristic: social reinforcement effect [7, 14], which usually plays a vital role in the final status of contagions.

To examine social reinforcement effect, some successful models have been proposed [15, 16], most of which assume that all individuals have the same adoption threshold to incorporate such an effect (so-called threshold model). That is to say, each individual adopts the behavior only when the fraction [15] or number [16] of neighbors with the adopted state exceeds his adoption threshold. In this case, the social contagions is a trivial case of Markovian process. By means of numerical simulations and theoretical analysis, it was found that the social reinforcement effect can evidently change the phase transitions of contagion dynamics. More specifically, the final adoption size first grows continuously and then decreases discontinuously with the increase of mean degree when the adoption threshold of all individuals is identical [15]. After this seminal discovery, the role of threshold model and

its various underlying mechanisms, in social contagions have been intensively explored, including the influence of dynamical parameters (e.g., initial seeds and threshold sizes [17, 18]), and topology characteristics (degree-degree correlations [19], clustering [20, 21], community structure [22] as well as multiplexity framework [23, 24]), which are the primary factors in determining the final adoption size and phase transition. Some non-Markovian social contagion models were also proposed to describe the social reinforcement effect [25–27]. For example, in a recent research paper [26], where the social reinforcement was derived from the memory of non-redundant information transmission, it was found that the perturbation of dynamical or structural parameters makes the dependence of final behavior adoption size on information transmission probability change from being discontinuous to being continuous. In Ref. [27], Zheng *et al.* further verified that the role of social reinforcement in behavior diffusion on regular graphs and online social networks, which is consistent with early experimental anticipation [28]

Recently, researchers found that the widely existed individual heterogeneity dramatically alters the spreading dynamics. In epidemic spreading, the heterogeneous infectivity and susceptibility can change the outbreak threshold [29, 30]. For information spreading, the heterogeneous waiting and response time may speed up or slow down the velocity of information diffusion [31, 32]. Statistical physicists found that individual heterogeneity can induce the hybrid phase transition [33, 34], which mixes the traditional first-order and second-order transitions, in k -core percolation [35] and bootstrap percolation [17, 36, 37]. In practical behavior spreading, individuals usually show different wills to mimic the behavior, which means that each agent owns his own adoption threshold [38]. Some individuals with low adoption threshold show strong wills to adopt the behavior and act as *activists*. Nevertheless, others with high adoption threshold need to capture more behavioral information before imitation, and they often

* tangminghuang521@hotmail.com

† zhenwang0@gmail.com

act as *bigots*. With regard to the difference of adoption threshold, it may be closely related with personal interests, education background, or other personality and social factors [1]. For example, the well-educated population is more likely to adopt the high-tech products than that among the populations who lacks the basic education. Similarly, students are more likely to adopt an interesting computer game than housewives.

Unfortunately, there is still absence of systematical understanding about the role of heterogeneous adoption thresholds in social contagions. Aiming to resolve this issue, we will explore how heterogeneous adoption thresholds affect the final adoption size and phase transition of social contagions based on a so-called binary spreading threshold model, which is a non-Markovian process. Meanwhile, an edge-based compartmental theory is developed for quantitative validation. Interestingly, it is found that heterogeneous adoption thresholds significantly affect the final adoption size, and generate the hierarchical characteristic of adopting behavior: activists first adopt the given behavior themselves, and then stimulate bigots to follow this behavior. Moreover, it is worth noting that such a heterogeneous threshold model results in the existence of first-order, second-order and hybrid phase transitions. More importantly, there are two different kinds of crossover phenomena in phase transition for distinct values of the bigots' adoption threshold: a change from first-order or hybrid phase transitions to the second-order phase transition. In what follows, we will first describe the heterogeneous social contagion model in complex networks, followed by the description of edge-based compartmental theory, and then represent the simulation and analysis results. Finally, we will draw our conclusions.

II. SOCIAL CONTAGION MODEL WITH HETEROGENEOUS ADOPTION THRESHOLDS

Behavior spreading on complex networks is considered with N nodes and the degree distribution $P(k)$. As the interaction networks, we use the configuration model [39] to avoid the additional influence of degree-degree correlations. Nodes in the network represent individuals and edges between nodes stand for the contacts with which behavioral information transmission may occur. For each individual, a static behavioral adoption threshold is assigned according to a specific distribution function $F(T)$, which is independent of network topology. The larger value of T means that an individual needs to capture more behavioral information from his neighbors before adopting the behavior.

With regard to behavior spreading dynamics, we generalize the spreading threshold model with social reinforcement derived from memory of non-redundant information transmission characters [26, 40]. In this model, each individual falls into one of the three states: susceptible (S), adopted (A) and recovered (R) (namely, susceptible-adopted-recovered, SAR model). In the susceptible state, an individual does not adopt the behavior. In the adopted state, an individual adopts the behavior and tries to transmit the behavioral information to his neighbors. In the recovered state, an individual loses interest

in the behavior and will not transmit the behavioral information further. Initially, a vanishingly small fraction of individuals ρ_0 are chosen as seeds (adopters) at random, while the others are fixed in the susceptible state.

At each time step, each adopted individual v tries to diffuse the behavioral information to every susceptible neighbor with probability λ . In particular, once the information is transmitted through an edge successfully, it will never be transmitted again, i.e., only non-redundant information transmission is allowed. If the susceptible neighbor u of v is successfully informed, his cumulative pieces of information m add 1 (i.e., $m = m + 1$). Subsequently, individual u compares the new value of m with his adoption threshold T_u , and becomes an adopter once $m \geq T_u$. Obviously, whether an individual adopts the behavior is determined by the cumulative pieces of behavioral information he ever received from distinct neighbors. Thus, the non-Markovian effect is induced in the behavior spreading dynamics. After information transmission, individual v may lose interest in the behavior with probability γ and then moves into the recovered state. Individuals falling into the recovered state will stop from participating in the further behavioral information spreading, and the spreading dynamics terminate when all adopted individuals become recovered.

III. EDGE-BASED COMPARTMENTAL THEORY

In order to describe the strong dynamical correlations among the states of neighbors in heterogeneous social contagion model, an edge-based compartmental approach is established herein, which is inspired by Refs. [41–43]. Correspondingly, the notations $S(t)$, $A(t)$ and $R(t)$ respectively represent the fraction of individuals in the susceptible, adopted, and recovered states at time step t .

A. General adoption threshold distribution

Individual u is set to be in the cavity state, which means that he can receive behavioral information from neighbors but not transmit behavioral information to his neighbors [44]. Define $\theta(t)$ as the probability that individual v has not transmitted the behavioral information to individual u along a randomly chosen edge by time t . Thus, the probability that an individual u with degree k has received m pieces of behavioral information from distinct neighbors by time t can be expressed as

$$\phi_m(k, t) = \binom{k}{m} [\theta(t)]^{k-m} [1 - \theta(t)]^m. \quad (1)$$

Individual u in the susceptible state implies that the cumulative pieces of behavioral information m he received are still less than his adoption threshold T_u . According to the social contagion model in Sec. II, the adoption threshold and degree are independent. Considering all possible values of m and T_u , it can be obtained that the probability of individual u with

degree k being susceptible is

$$s(k, t) = \sum_{T_u} F(T_u) \sum_{m=0}^{T_u-1} \phi_m(k, t). \quad (2)$$

Combing the degree distribution of a network, the fraction of susceptible individuals at time step t is

$$S(t) = \sum_k P(k) s(k, t). \quad (3)$$

It is obvious that $S(t)$ can be figured out after $\theta(t)$ is known.

As a neighbor of individual u may be in one of susceptible, adopted or recovered state, $\theta(t)$ can be divided into three cases as

$$\theta(t) = \xi_S(t) + \xi_A(t) + \xi_R(t). \quad (4)$$

And $\xi_S(t)$ [$\xi_A(t)$ or $\xi_R(t)$] denotes that the susceptible (adopted or recovered) neighbor v of u has not transmitted the behavioral information to individual u up to time t .

Then, let's explore the above three terms. If individual v with degree k' is susceptible initially, he can not transmit the behavioral information to u , but only receive it from other $k' - 1$ neighbors since u in a cavity state. Thus, the probability that individual v has received m pieces of behavioral information by time t is

$$\tau_m(k', t) = \binom{k' - 1}{m} [\theta(t)]^{k' - m - 1} [1 - \theta(t)]^m. \quad (5)$$

Taking all possible values of m and T_v into consideration, the probability of individual v remaining in susceptible state becomes [similar to Eq. (2)]

$$\Theta(k', t) = \sum_{T_v} F(T_v) \sum_{m=0}^{T_v-1} \tau_m(k', t). \quad (6)$$

The probability of an edge connecting an individual with degree k' is $k'P(k')/\langle k \rangle$ for uncorrelated networks, where $\langle k \rangle$ is the mean degree. Thus, it can be obtained that

$$\xi_S(t) = \frac{\sum_{k'} k' P(k') \Theta(k', t)}{\langle k \rangle}. \quad (7)$$

Subsequently, we turn to the expressions of $\xi_A(t)$ and $\xi_R(t)$. Once the behavioral information is transmitted through an edge with probability λ , the edge will no longer satisfy the definition of $\theta(t)$. Thus, the rate of flow from $\theta(t)$ to $1 - \theta(t)$ is $\lambda \xi_A(t)$, which can be expressed as

$$\frac{d\theta(t)}{dt} = -\lambda \xi_A(t). \quad (8)$$

For the growing of $\xi_R(t)$, two events conditions must be met simultaneously. At time t , the behavioral information does not transmit through an edge with probability $1 - \lambda$, and the adopted individual enters recovered state with probability γ . Then,

$$\frac{d\xi_R(t)}{dt} = \gamma(1 - \lambda)\xi_A(t). \quad (9)$$

Combining Eqs. (8) and (9), one has that

$$\xi_R(t) = \frac{\gamma[1 - \theta(t)](1 - \lambda)}{\lambda}. \quad (10)$$

Inserting Eqs. (7) and (10) into Eq. (4), the following expression can be obtained that

$$\xi_A(t) = \theta(t) - \frac{\sum_{k'} k' P(k') \Theta(k', t)}{\langle k \rangle} - \frac{\gamma[1 - \theta(t)](1 - \lambda)}{\lambda}. \quad (11)$$

Substituting Eq. (11) into Eq. (8), we get the time evolution of $\theta(t)$ in details

$$\frac{d\theta(t)}{dt} = -\lambda[\theta(t) - \frac{\sum_{k'} k' P(k') \Theta(k', t)}{\langle k \rangle}] + \gamma[1 - \theta(t)](1 - \lambda). \quad (12)$$

Susceptible individuals move into the adopted states once they adopt the behavior, meanwhile the adopted individuals may lose interest in the behavior and become recovered. Thus, we can easily get the evolution of adopted and recovered individuals as

$$\frac{dA(t)}{dt} = -\frac{dS(t)}{dt} - \gamma A(t) \quad (13)$$

and

$$\frac{dR(t)}{dt} = \gamma A(t), \quad (14)$$

respectively. Eqs. (1)-(3) and (12)-(14) give us a complete and general description of heterogeneous social contagions, from which the fraction in each state at arbitrary time step can be calculated. When $t \rightarrow \infty$, we can get the final adoption size $R(\infty)$.

B. Binominal adoption threshold distribution

In this subsection, we pay attention to the behavior adoption threshold with a binominal distribution $F(T)$. More specifically, a fraction of individuals p have a relatively low adoption threshold T_a , whereas the remaining individuals have a high adoption threshold T_b . $F(T)$ can be expressed as

$$F(T) = \begin{cases} T_a, & \text{with probability } p, \\ T_b, & \text{with probability } 1 - p. \end{cases} \quad (15)$$

For simplicity, the values of adoption thresholds are defined as $T_a = 1$ and $T_b \geq 1$. Individuals with low adoption threshold T_a are considered as *activists*, while those with high adoption threshold T_b are regarded as *bigots*. We herein name this kind of social contagion model as *binary spreading threshold model*. And the edge-based compartmental theory is utilized to analyze the binary spreading threshold model by substituting Eq. (15) into various equations that give the solutions of $S(t)$, $A(t)$ and $R(t)$. Particularly, we rewrite Eqs. (2) and (6) as

$$s(k, t) = p\theta(t)^k + (1 - p) \sum_{m=0}^{T_b-1} \phi_m(k, t), \quad (16)$$

and

$$\Theta(k', t) = p\theta(t)^{k'-1} + (1-p) \sum_{m=0}^{T_b-1} \tau_m(k', t), \quad (17)$$

respectively. At time t , the fractions of susceptible individuals in the activist and bigot populations are given by

$$S_l(t) = \sum_k P(k)\theta(t)^k, \quad (18)$$

and

$$S_h(t) = \sum_k P(k) \sum_{m=0}^{T_b-1} \phi_m(k, t), \quad (19)$$

respectively. Considering the fractions of the activist and bigot populations, the density of susceptible individuals at time step t can also be written as

$$S(t) = pS_l(t) + (1-p)S_h(t). \quad (20)$$

The effects of heterogeneous adoption threshold on phase transition is another issue concerned. To analyze the phase transition, we can address the fixed point (root) of Eq. (12) at the steady state (i.e., $t \rightarrow \infty$) with Eq. (17). That is the fixed point of

$$\theta(\infty) = y[\theta(\infty)], \quad (21)$$

where

$$y[\theta(\infty)] = \frac{\sum_{k'} k' P(k') \Theta(k', \infty)}{\langle k \rangle} + \frac{\gamma[1 - \theta(\infty)](1 - \lambda)}{\lambda}. \quad (22)$$

From Fig. 1(a), it can be seen that the number of nontrivial roots is either 0, 1 or 3 when $T_b \geq 3$. With $T_b = 2$, the number of nontrivial roots is either 0, 1 or 2 [see Fig. 1(b)].

1. Case of $T_b \geq 3$

In this subsection, we discuss the case of $T_b \geq 3$. For the given $P(k)$, p and γ , Eq. (21) has only one trivial solution $\theta(\infty) = 1$ when λ is small. With the increase of λ , $\theta(\infty)$ decreases continuously to a nontrivial solution $\theta(\infty) < 1$ first [see example in Fig. 1(a)], which means that $R(\infty)$ grows continuously first. That is to say, there is a second-order (continuous) phase transition. By setting $\theta(\infty)$ and $y[\theta(\infty)]$ tangent at $\theta(\infty) = 1$ [34, 45], we get the continuous critical information transmission probability as

$$\lambda_c^{II} = \frac{\gamma \langle k \rangle}{p(\langle k^2 \rangle - \langle k \rangle) - (1 - \gamma)\langle k \rangle}, \quad (23)$$

where $\langle k \rangle$ and $\langle k^2 \rangle$ are the first and second moments of degree distribution, respectively. The critical value λ_c^{II} separates the local behavior adoption (i.e., the behavior can be adopted by a vanishingly small fraction of individuals) from the global

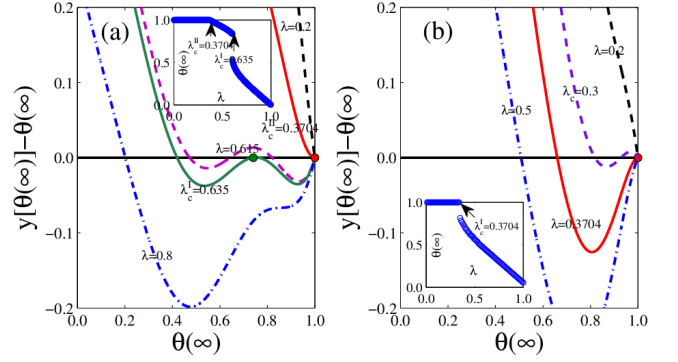


FIG. 1. (Color online) Illustration of graphical solutions of Eq. (21) when $T_b = 4$ (a) and $T_b = 2$ (b) on random regular networks. In (a) and (b), the black solid lines represent the horizontal axis and the red and green dots denote the tangent points. The inset of (a) and (b) shows the physically meaningful solutions of Eq. (21) when $T_b = 4$ and $T_b = 2$, respectively. And the arrows indicate critical transmission probabilities. The fixed points of Eq. (21) are the intersections between the curve and horizontal axis. Other parameters are defined $p = 0.3$ and $\langle k \rangle = 10$.

behavior adoption (i.e., the behavior can be adopted by a finite fraction of individuals). From Eq. (23), it is discovered that the occurrence of global behavior adoption is determined by the network topology (i.e., degree distribution), the fraction of activists p and the recovery probability γ . The global behavior adoption is more likely outbreak (i.e., a lower λ_c^{II}) for scale-free networks with divergent second moment degree distribution [i.e., $\langle k^2 \rangle \rightarrow \infty$]. Increasing the value of p can facilitate the global behavior adoption (i.e., a lower λ_c^{II}). When $p = 1$, Eq. (23) returns to the case of epidemic outbreak threshold [43].

Fixing all the parameters except p , similar to Eq. (23), we get the continuous critical fraction of activists as

$$p_c^{II} = \frac{\gamma \langle k \rangle}{\lambda(\langle k^2 \rangle - \langle k \rangle)} + \frac{(1 - \gamma)\langle k \rangle}{\langle k^2 \rangle - \langle k \rangle}. \quad (24)$$

From Eq. (24), it can be known that an enough fraction of activists are necessary for triggering the global behavior adoption, and p_c^{II} decreases with the increase of network heterogeneity, p and λ . By setting $\gamma = 0$ in Eq. (24), another critical proportion of activists p_c^* can be obtained, below which any values of λ can not trigger the global behavior adoption, which is given by

$$p_c^* = \frac{\langle k \rangle}{\langle k^2 \rangle - \langle k \rangle}. \quad (25)$$

It is worth noting that Eq. (25) is the same with network's percolation condition [45], which means that the global behavior adoption is possible only when the activists percolate the entire network (i.e., activists can form a finite connected cluster).

As shown in Fig. 1(a), three nontrivial roots of Eq. (21) occur when λ is large enough [see Fig. 1(a) for $\lambda = 0.615$].

This phenomenon is caused by the bigots, since Eq. (21) has at most one nontrivial root when the bigots is absent [26]. In this case, the meaningful solution will be given by the largest stable root (since only this value can be achieved physically). For $\lambda = \lambda_c^I = 0.635$, the tangent point is the solution. For $\lambda > \lambda_c^I$, the meaningful solution is the only stable fixed point. The meaning solution of Eq. (21) changes abruptly to a small value from a relatively large value at λ_c^I [see the insert Fig. 1(a)], and resulting in a discontinuous growth of $R(\infty)$. Based on bifurcation theory [46], the discontinuous critical information transmission probability is gained as follows

$$\lambda_c^I = \frac{\gamma}{\Delta + \gamma - 1}, \quad (26)$$

where

$$\Delta = \frac{\sum_{k'} k' P(k') \frac{d\Theta(k', \infty)}{d\theta(\infty)} |_{\theta_s(\infty)}}{\langle k \rangle},$$

and $\theta_s(\infty)$ is the fixed point of Eq. (21). Combining Eqs. (5) and (17), we get

$$\frac{d\Theta(k', \infty)}{d\theta(t)} = p(k' - 1)\theta(\infty)^{k'-2} + (1 - p)\mathcal{X}, \quad (27)$$

where

$$\mathcal{X} = \sum_{m=0}^{T_b-1} \binom{k' - 1}{m} \{ (k' - m - 1)\theta(\infty)^{k'-m-2} [1 - \theta(\infty)]^m - m\theta(\infty)^{k'-m-1} [1 - \theta(\infty)]^{m-1} \}. \quad (28)$$

Using the analytical method similar to Eq. (26), the discontinuous critical fraction of activists can be expressed as

$$p_c^I = \frac{\lambda(1 - \mathcal{Y}) + \gamma(1 - \lambda)}{\lambda(\mathcal{Z} - \mathcal{Y})}, \quad (29)$$

where

$$\mathcal{Y} = \frac{\sum_{k'} k' P(k') \mathcal{X}}{\langle k \rangle}$$

and

$$\mathcal{Z} = \frac{\sum_{k'} k' (k' - 1) P(k') \theta^{k'-2}}{\langle k \rangle}.$$

From the above analysis, we find that $R(\infty)$ versus λ or p first grows continuously and then follows a discontinuous fashion. And the continuous and discontinuous growths of $R(\infty)$ are caused by the activists and bigots, respectively, which can be regarded as hybrid phase transition, mixing the traditional first-order and second-order transitions, from the perspective of statistical physics [47]. Note that the hybrid phase transition can change to a second-order phase transition, and does not exist under any conditions. Numerically solving Eqs. (21), (26), and the following equation

$$\frac{d^2 g[\theta(\infty)]}{d\theta^2(\infty)} = 0, \quad (30)$$

we can learn the condition under which the hybrid phase transition disappears.

2. Case of $T_b = 2$

We study the special case of $T_b = 2$ in this subsection. As shown in Fig. 1(b), for any λ , $y[\theta(\infty)]$ can only tangent to $\theta(\infty)$ when $\theta(\infty) = 1$, and can not tangent to other $\theta(\infty) < 1$. In addition, Eq. (21) has 1 or 2 nontrivial fixed points. These phenomena means that the meaningful solution of Eq. (21) jumps to another one at the critical information transmission probability [see the inset of Fig. 1(b)]. As a result, $R(\infty)$ increases discontinuously versus λ . The critical information transmission probability can be acquired in the similar way as when $T_b = 3$. The values of λ_c^{II} and λ_c^I can be obtained from Eq. (23), since $y[\theta(\infty)]$ can only tangent to $\theta(\infty)$ when $\theta(\infty) = 1$. Numerical solving Eqs. (21), (26) and (30), we can get the condition under which the first-order phase transition changes to a second-order phase transition.

IV. NUMERICAL VERIFICATION

In the study, extensive simulations are conducted for on binary spreading threshold model on uncorrelated networks. Unless otherwise specified, the network size, mean degree and recovery probability are of $N = 10,000$, $\langle k \rangle = 10$ and $\gamma = 1.0$, respectively. At least 2×10^3 independent dynamical realizations on a fixed network are used to calculate the pertinent average values, which are further averaged over 100 network realizations.

The *relative variance* v_R is applied to numerically determine the size-dependent critical values, such as, λ_c^I , λ_c^{II} , p_c^I and p_c^{II} . The relative variance of $R(\infty)$ is defined as

$$v_R = \frac{\langle R(\infty) - \langle R(\infty) \rangle \rangle^2}{\langle R(\infty) \rangle^2}, \quad (31)$$

where $\langle \dots \rangle$ denotes ensemble averaging. The value of v_R exhibits peaks at the phase transition, which announce the phase transition [48]. We determine the critical value ω_c , which represents λ_c^I , λ_c^{II} , p_c^I or p_c^{II} , as the value of λ or p when the relative variance reaches its maximum, and

$$\omega_c = \arg\{\max v_R\}. \quad (32)$$

Note that Eq. (32) is not the only possible way to compute the critical values, other methods can be used to determine ω_c , such as, susceptibility [49, 50] and variability [51].

A. Random regular networks

To be illustrative, we first focus on random regular networks (RRNs). Fig. 2(a) shows the time evolution of the fraction of adopted individuals $A_a(t)$ and $A_b(t)$ in the activist and bigot populations with different behavioral information transmission probabilities λ . It is found that a hierarchical character of behavior adoption is caused by heterogeneous adoption thresholds. That is to say, activists with low T_a first adopt the behavior and then stimulate the bigots with T_b to

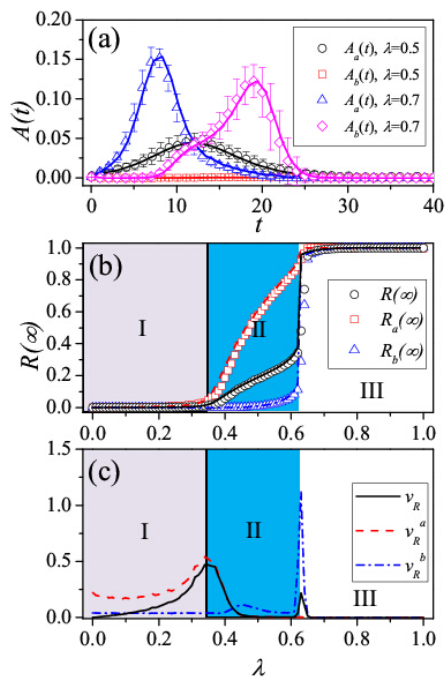


FIG. 2. (Color online) Binary spreading threshold model on random regular networks. (a) Average density of adopted individuals $A_a(t)$ and $A_b(t)$ versus time t in the activist and bigot populations with different information transmission probability λ . The error bars indicate the standard deviations. (b) Final adoption size $R(\infty)$ and (c) relative variance v_R versus λ for full, activist and bigot populations. In figures (a) and (b), symbols represent the simulated results, and the lines are the corresponding theoretical predictions from Eqs. (12)-(14) and (16)-(20). Lines in (c) are the simulation results of v_R . In (b) and (c), the vertical lines are the critical continuous and discontinuous information transmission probabilities, which are denoted as λ_c^{II} and λ_c^I , respectively. The theoretical values of λ_c^{II} and λ_c^I can be gotten from Eqs. (23) and (26), respectively. The theoretical (numerical) values of λ_c^{II} and λ_c^I separate (b) [(c)] into three regions. Region I, only a vanishingly small fraction of individuals can be exposed to adopt the behavior; region II, only a finite fraction of activists adopt the behavior; region III, a finite fraction of activists and bigots adopt the behavior. Other parameters are set to be $N = 10,000$, $p = 0.3$ and $T_b = 4$.

adopt the behavior. With a relatively small $\lambda = 0.5$, $A_a(t)$ shows a small peak, and can not stimulate a finite fraction of bigots to adopt the behavior [$A_b(t)$ does not see an obvious peak]. With a relatively large $\lambda = 0.7$, $A_a(t)$ shows a large peak, and further causing the emergence of a large peak for $A_b(t)$. The heterogeneous adoption threshold distribution may be used to explain the existence of multimodal in the adoption of serves [38]. The time evolution can be well predicted by our edge-based compartmental theory.

From Figs. 2(b) and (c), it can be seen that $R(\infty)$ versus λ shows a hybrid phase transition, which means that $R(\infty)$ first grows continuously and then follows a discontinuous fashion. The continuous and discontinuous phase transitions are caused by activists and bigots, respectively. Similar to

Ref. [26], the discontinuous growth of $R(\infty)$ is caused by those bigots in the subcritical state who adopt the behavior simultaneously. An individual in such a state has received the behavioral information but has not yet adopted the behavior, and the number of information pieces from distinct neighbors is precisely one less than his adoption threshold. The theoretical (numerical) values of λ_c^{II} and λ_c^I separate Figs. 2(b) [(c)] into three regions. The theoretical values of λ_c^{II} and λ_c^I can be gotten from Eqs. (23) and (26), respectively. In region I, with $\lambda \leq \lambda_c^{II}$, both activist and bigot populations adopt the behavior locally (i.e., only a vanishingly small fraction of individuals adopted the behavior). In region II, with $\lambda_c^{II} < \lambda \leq \lambda_c^I$, activists adopt the behavior globally (i.e., a finite fraction of activists adopted the behavior) and bigots adopt the behavior locally. In region III with $\lambda > \lambda_c^I$, both the activists and bigots adopt the behavior globally. The numerical values of λ_c^{II} and λ_c^I can be obtained by observing v_R in Fig. 2(c). For instance, v_R has two peaks, which means that two phase transitions occur [48]. And the first peak appears at λ_c^{II} , while the second peak locates at λ_c^I . Note that the first (second) peak of v_R shares the same location with the maximal peak of activist population v_R^a (bigots population v_R^b). In all, λ_c^{II} , λ_c^I and $R(\infty)$ can be well predicted by our edge-based compartmental theory.

As shown in Fig. 3, $R(\infty)$ and the phase transition are significantly influenced by the adoption threshold of bigots T_b . And $R(\infty)$ decreases with T_b , since a larger value of T_b requires more information to be exposed for bigots. The phase transition is continuous when $T_b = 1$. In this case, the contagion dynamics is the same with epidemic spreading [45]. The phase transition is also continuous when $T_b \geq 6$, since there are not enough activists to persuade bigots to adopt the behavior simultaneously. For the case of $T_b = 2$, $R(\infty)$ shows a first-order phase transition, because the bigots are likely to enter subcritical states and adopt the behavior simultaneously. A hybrid phase transition emerges with other values of T_b (i.e., $2 < T_b < 6$). As discussed in Sec. III B, the type of phase transition is verified by bifurcation analysis of Eq. (21). In Fig. 3(b), we verify the phase transition by studying v_R in simulations. And the simulated values of λ_c^{II} and λ_c^I are located by studying v_R versus λ . For the second-order phase transition, v_R has only one peak [see $T_b = 1$ and $T_b = 6$ in Fig. 3(c)]. Similarly, v_R also has only one peak for the first-order phase transition [see $T_b = 2$ in Fig. 3(c)]. For the hybrid phase transition, v_R has two peaks [see $3 \leq T_b \leq 5$ in Fig. 3(c)]. Our theoretical predictions of $R(\infty)$ are well agree with the simulation results, except for the cases near the critical information transmission probability. The deviations between our predictions and simulation are mainly derived from the finite-size effects of the networks, as shown in Fig. 4. The deviations of $R(\infty)$, λ_c^I and λ_c^{II} between the simulated and theoretical results decrease with network size N .

Then, we observe $R(\infty)$ versus p for different λ in Fig. 5. We find that $R(\infty)$ increases with p . By bifurcation analysis of Eq. (21) and studying v_R , a continuous growth of $R(\infty)$ is observed with a relatively small λ (e.g., $\lambda = 0.5$), and the hybrid phase transition occurs with a relatively large λ (e.g., $\lambda = 0.7$ and 0.8). Again, the theoretical and numerical results

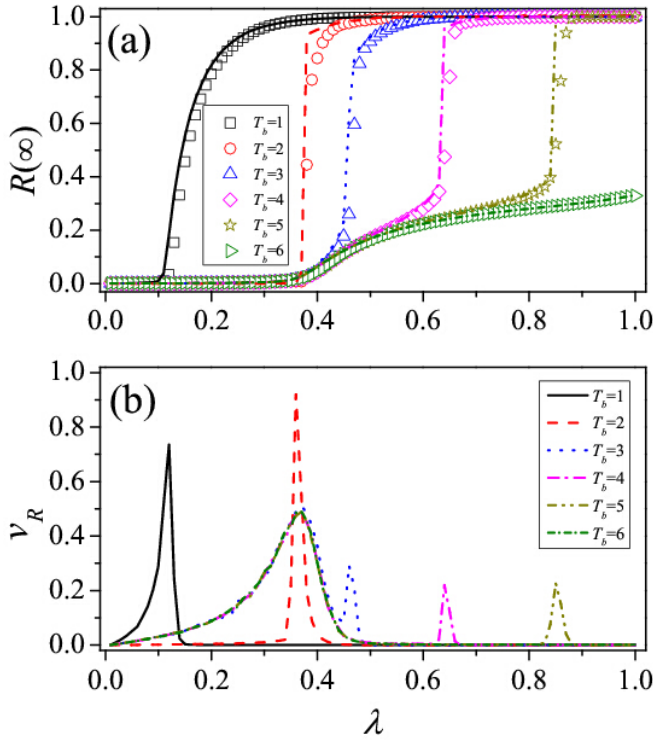


FIG. 3. (Color online) Effects of bigots' adoption threshold on binary spreading threshold model. (a) $R(\infty)$ and (b) v_R versus λ with different T_b . In figure (a), symbols represent the simulated results, and the lines are the theoretical predictions from Eqs. (12)-(14) and (16)-(20). In figure (b), lines are the simulation results of v_R , and we plot the value of $v_R/20$ for $T_b = 2$. Other parameters are defined as $N = 10,000$ and $p = 0.3$.

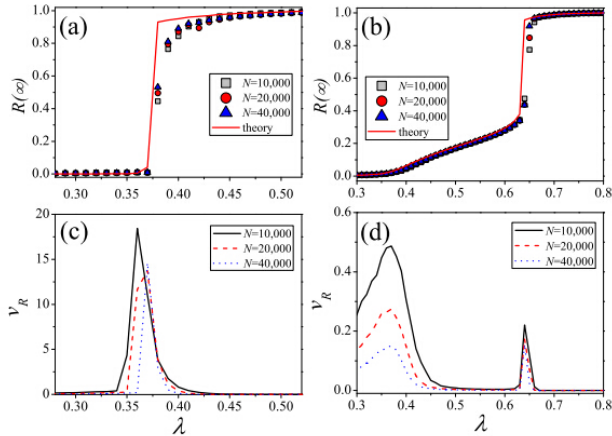


FIG. 4. (Color online) Finite-size effects on the binary spreading threshold model for $p = 0.3$. (a) $R(\infty)$ and (c) v_R versus λ for $T_b = 2$ on different network size N . (b) $R(\infty)$ and (d) v_R versus λ for $T_b = 4$ under different N . The lines in (a) and (b) are the theoretical predictions from Eqs. (12)-(14) and (16)-(20). The lines in (c) and (d) are the simulation results of v_R .

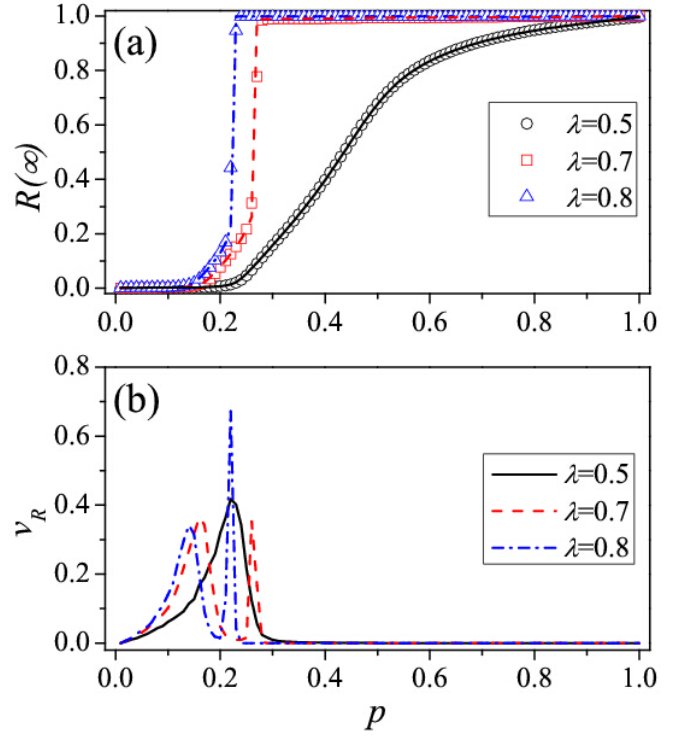


FIG. 5. (Color online) Effects of the fraction of activists on binary spreading threshold model. (a) $R(\infty)$ and (b) v_R as a function of p for different λ . In figure (a), symbols represent the simulated results, and the lines are the theoretical predictions from Eqs. (12)-(14) and (16)-(20). Lines in (b) are the simulation results of v_R . We set other parameters to be $N = 10,000$ and $T_b = 4$.

agree well.

From the above analysis, it can be obtained that both λ and p markedly affect $R(\infty)$ and phase transition. Thus, we further investigate $R(\infty)$ and phase transition on parameter plane (λ, p) when $T_b = 4$ in Fig. 6. Obviously, $R(\infty)$ increases with λ and p . According to the type of phase transition, the parameter plane (λ, p) is divided into four different regions by three vertical lines. The first vertical line can be gotten from Eq. (25), and the other two can be predicted by solving Eqs. (21), (26) and (30). In region I ($p \leq p_c^* = 1/9$), there are a few activists, who can not percolate the entire population. Thus, no matter what the value of λ , activists can not be made to adopt the behavior globally. When $p > p_c^*$, the global behavior adoption becomes possible, and a crossover phenomenon, which means that the phase transition changes from being hybrid to being second-order, occurs in the phase transition. Meanwhile, the local and global behavior adoptions are separated by the red solid curve (i.e., λ_c^{II}). In region II ($1/9 < p \leq 0.15$), the relatively few activists lead to the continuous phase transition. In this region, $R(\infty)$ grows continuously versus λ for a given p , and a finite fraction of individuals adopt the behavior above λ_c^{II} . With the increase of p , in region III ($0.15 < p < 0.5$), the hybrid phase transition occurs, i.e., $R(\infty)$ first grows continuously with λ and then follows by a discontinuous pattern. A finite fraction of activists adopt the

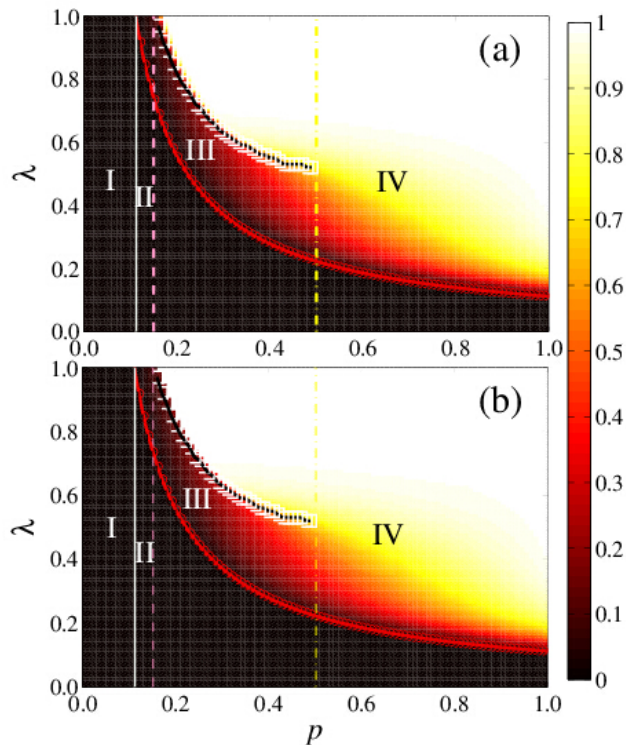


FIG. 6. (Color online) Dependence of $R(\infty)$ on p and λ on random regular networks. Color-coded values $R(\infty)$ are obtained from numerical simulations (a) and theoretical solutions (b) in the parameter plane (p, λ) , and the theoretical predictions are the solutions of Eqs. (12)-(14) and (16)-(20). The plane are divided into four regions by three vertical lines, of which the first line can be gotten from Eq. (25) and the other two are predicted by solving Eqs. (21), (26) and (30). In region I, only a vanishingly small fraction of individuals can be exposed to adopt the behavior (i.e., local behavior adoption). Both the regions II and IV show a continuous phase transition, while region III exhibits a hybrid phase transition. The red circles (red solid curve) and white squares (black dashed curve) are the continuous and discontinuous simulated (theoretical) critical information transmission probability, respectively. Moreover, other parameters defined as $N = 10,000$, $p = 0.3$ and $T_b = 4$.

behavior above λ_c^{II} , and further induce the bigots to adopt the behavior simultaneously above λ_c^I [see black curves obtained from Eq. (26)]. In region IV ($p \geq 0.5$), half of the neighbors of bigots are activists. Once these activists adopt the behavior, the bigots will gradually adopt the behavior. Thus, $R(\infty)$ grows continuously and a finite fraction of individuals adopt the behavior above λ_c^{II} (see red curves). Our theoretical predictions of λ_c^{II} , λ_c^I and $R(\infty)$ have a good agreement with the numerical predictions.

It can be seen in Fig. 3 that $R(\infty)$ increases discontinuously with λ when $T_b = 2$, thus $R(\infty)$ and phase transition on parameter plane (p, λ) for $T_b = 2$ is explored in Fig. 7. And we find another crossover phenomenon in the phase transition: a change from being first-order to being second-order. Similar to Fig. 6 is that the plane is divided into three regions: Region I ($p \leq 1/9$), the local behavior adoption region, in which

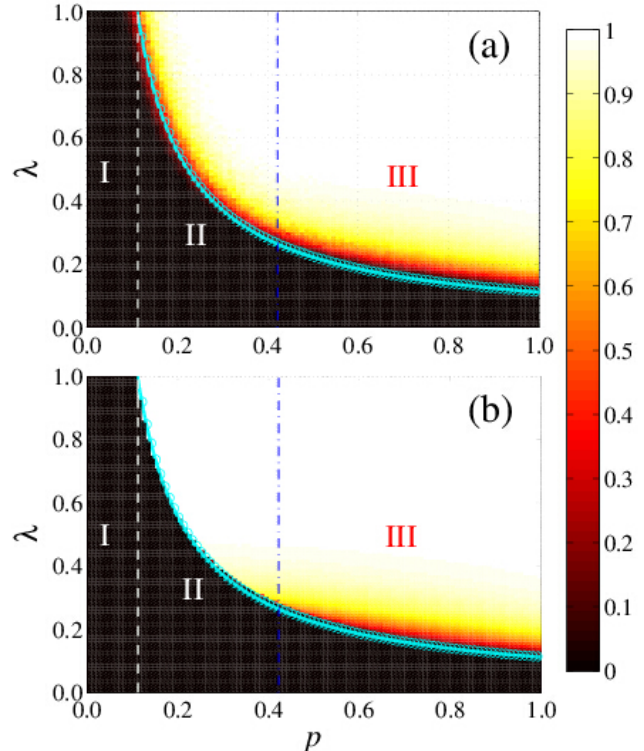


FIG. 7. (Color online) Dependence of $R(\infty)$ on p and λ . Color-coded values $R(\infty)$ from numerical simulations (a) and theoretical solutions (b) in the parameter plane (p, λ) , and the theoretical predictions are the solutions of Eqs. (12)-(14) and (16)-(20). Two vertical lines separate the plane into three regions, the former line is predicted by Eq. (25) and the latter line is predicted by numerically solving Eqs. (21), (26) and (30). In region I, only a vanishingly small fraction of individuals can be exposed to adopt the behavior (i.e., local behavior adoption). Region II shows a discontinuous phase transition, while region III exhibits a continuous phase transition. The blue circles (blue dashed solid curve) are the simulated (theoretical) critical information transmission probability, respectively. We set other parameters as $N = 10,000$, $p = 0.3$ and $T_b = 2$.

only a vanishingly small fraction of individuals adopt the behavior; region II ($1/9 < p \leq 0.42$) shows a first-order phase transition, where a finite fraction of individuals adopt the behavior simultaneously above λ_c^I (red dashed lines); region III ($p > 0.42$) exhibits a second-order phase transition, in which $R(\infty)$ increases continuously versus λ . The type of phase transition is verified by bifurcation analysis and studying v_R .

B. Heterogeneous networks

We turn to elucidate the effects of network heterogeneity. To build the heterogeneous networks, the uncorrelated configuration model with power-law degree distributions $P(k) \sim k^{-\gamma_D}$ is adopted, where the mean degree $\langle k \rangle = 10$ and the maximum degree $k_{max} \sim \sqrt{N}$ [39]. The network heterogeneity increases with the decrease of γ_D .

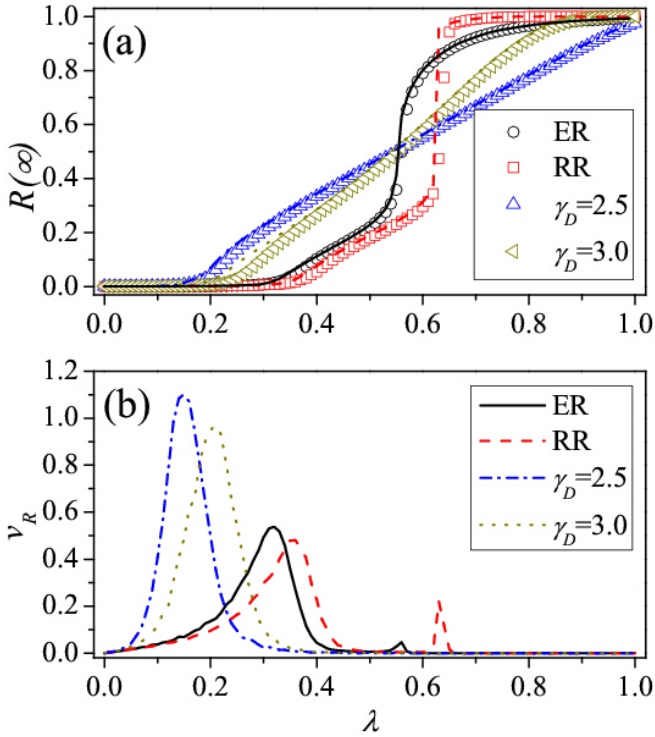


FIG. 8. (Color online) For $T_b = 4$, the effects of network heterogeneity on binary spreading threshold model. (a) $R(\infty)$ and (b) v_R versus λ on random regular networks, Erdős-Rényi (ER) networks, and scale-free networks with degree exponent $\gamma_D = 2.5$ and 3.0. In figure (a), symbols represent the simulated results, and the lines are theoretical predictions from Eqs. (12)-(14) and (16)-(20). Lines in (b) are the simulation results of v_R . We set other parameters to be $N = 10,000$ and $p = 0.3$.

In the case of $T_b = 4$, we find that the global behavior adoption more likely to occur (i.e., lower λ_c^{II}) in heterogeneous networks, due to the existence of hubs in heterogeneous networks [52], as shown in Fig. 8. Meanwhile, in strong heterogeneous networks a large number of individuals with small degrees are difficult to adopt the behavior, so $R(\infty)$ is smaller at large λ . For example, $R(\infty)$ at $\lambda = 0.7$ is obviously smaller on scale-free networks with $\gamma_D = 2.5$ than that on RRNs. By bifurcation analysis of Eq. (21), it is discovered that the hybrid phase transition disappears for strong heterogeneous networks (e.g., $\gamma_D = 2.5$ and 3.0 in Fig. 8). That is to say, network heterogeneity leads to the crossover phenomenon: a change from being hybrid to being second-order. Moreover, the type of phase transition is further verified by observing v_R in Fig. 8(b). Evidences in terms of the quantities $R(\infty)$, λ_c^I and λ_c^{II} support our edge-based compartmental theory.

For the case of $T_b = 2$ (see Fig. 9), we find the similar phenomenon of $R(\infty)$: $R(\infty)$ increases (decreases) with network heterogeneity for small (large) λ . However, the system has the first-order phase transition, which denotes that network heterogeneity does not alter the phase transition. Based on the bifurcation theory and the study of v_R , the phase transition is

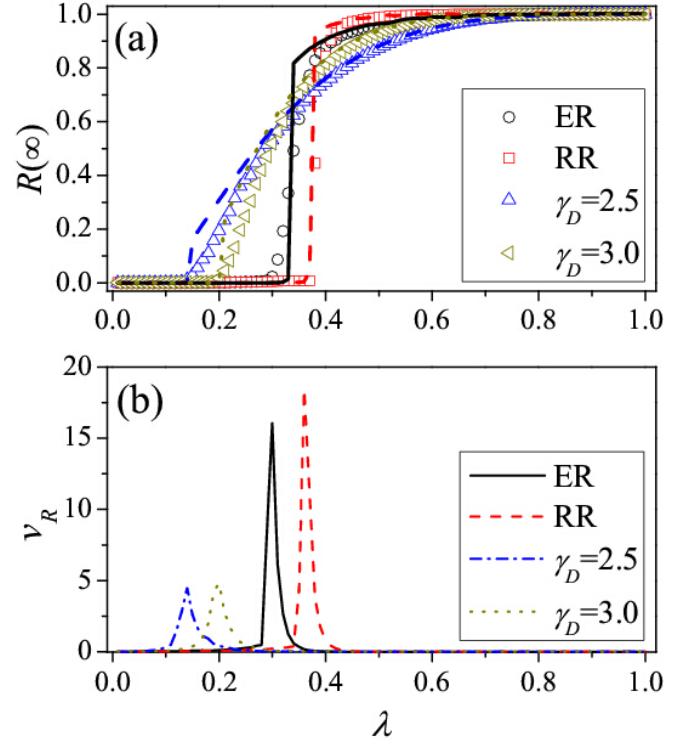


FIG. 9. (Color online) For $T_b = 2$, the effects of network heterogeneity on binary spreading threshold model. (a) $R(\infty)$ and (b) v_R versus λ on random regular networks, Erdős-Rényi (ER) networks, and scale-free networks with degree exponent $\gamma_D = 2.5$ and 3.0. In figure (a), symbols represent the simulated results, and the lines are the theoretical predictions from Eqs. (12)-(14) and (16)-(20). Lines in (b) are the simulation results of v_R . And other parameters are set to be $N = 10,000$ and $p = 0.3$.

verified [see Fig. 9(b)].

V. CONCLUSIONS

Understanding social contagion dynamics in human populations is extremely challenging. In practical behavior spreading, individuals usually display different criteria (wills) to adopt the behavior. That is to say, the heterogeneity of adoption thresholds do indeed exist, but its effects on social contagions have not been verified straightforward. To fill this gap, we proposed a non-Markovian behavior spreading model, in which individuals have distinct adoption thresholds, to explore how heterogeneous adoption thresholds affect the final adoption size and phase transition. An edge-based compartmental theory is developed to quantitatively describe this model, and this suggested theory is verified by a large number of simulations. In the paper, we mainly focused on the so-called binary spreading threshold model, in which a fraction of individuals p have the adoption threshold $T_a = 1$ and are acted as activists, and the remaining ones have a higher adoption threshold T_b and are regarded as bigots.

We first studied the spreading dynamics on random regular networks. And it is found that heterogeneous adoption thresholds markedly affect $R(\infty)$, and induce a hierarchical character in behavior adoption. In other words, activists first adopt the behavior and then stimulate bigots to adopt the behavior. All the first-order, second-order and hybrid phase transitions are found to be in existence in the system. For the case of $T_b = 1$, the traditional second-order phase transition can be found. For $T_b \geq 3$, the hybrid phase transition mixed first and second order, i.e., $R(\infty)$ versus λ first grows continuously and then follows by a discontinuous pattern, also occurs. More specifically, the continuous and discontinuous growth of $R(\infty)$ are caused by the activists and bigots, respectively. There is a crossover phenomenon between the hybrid and second-order phase transitions by varying p . When $T_b = 2$, the system only exhibits the first-order or second-order phase transitions. Interestingly, there is another crossover phenomenon: by varying p the phase transition changes from being first-order to being second-order.

Finally, we found that network heterogeneity markedly affects $R(\infty)$ and phase transition due to the existence of hub individuals. For the case of $T_b \geq 3$, strong network heterogeneity causes the phase transition to change from being hybrid to being second-order. For $T_b = 2$, network heterogeneity does not alter the type of phase transition.

The main contribution of our work lies in providing a quali-

tative and quantitative view on the influence of heterogeneous adoption threshold. Meanwhile, our research results also enrich the phase transition phenomenon. The developed theory can be generalized to behavior spreading with general adoption threshold distribution, and offer some new inspirations for other similar spreading dynamics, such as epidemic spreading and cascading. However, some fascinating and hopeful challenges still remain. For example, what will happen if the adoption thresholds are correlated with their degrees? How to extract more realistic behavior spreading mechanisms from real data?

ACKNOWLEDGEMENTS

This work was partially supported by the National Natural Science Foundation of China under Grants Nos. 11105025 and 11575041, the Program of Outstanding Ph. D. Candidate in Academic Research by UESTC under Grand No. YXB-SZC20131065.

REFERENCES

-
- [1] Watts D J and Dodds P S 2007 *Journal of Consumer Research*, **34** 441.
 - [2] Castellano C, Fortunato S and Fortunato S 2009 *Rev. Mod. Phys.* **81** 0034.
 - [3] Christakis N A and Fowler J H 2007 *N. Engl. J. Med.* **357** 370.
 - [4] Barrat A, Barthélemy M, and Vespignani A 2007 *Dynamical Processes on Complex Networks* (Cambridge: Cambridge University Press).
 - [5] Centola D 2011 *Science* **334** 1269.
 - [6] Banerjee A, Chandrasekhar A G, Duflo E and Jackson M O 2013 *Science* **341** 363.
 - [7] Pastor-Satorras R, Castellano C, Mieghem P V and Vespignani A 2014 arXiv:1408.2701v1.
 - [8] Moreno Y, Pastor-Satorras R and Vespignani A 2002 *Eur. Phys. J. B* **26** 521.
 - [9] Pastor-Satorras R and Vespignani A 2001 *Phys. Rev. Lett.* **86** 3200.
 - [10] Salathé M and Khandelwal S 2011 *PLOS Comput. Biol.* **7** e1002199.
 - [11] Yang H X, Tang M, and Lai Y C 2015 *Phys. Rev. E* **91** 062817.
 - [12] Yang H X, Wang W X, Lai Y C, Xie Y B, and Wang B H 2011 *Phys. Rev. E* **84** 045101(R).
 - [13] Li K, Fu X, Small M, and Zhu G 2014 *Chaos* **24** 043124.
 - [14] Porter M A and Gleeson J P 2014 arXiv:1403.7663v1.
 - [15] Watts D J 2002 *Proc. Natl. Acad. Sci.* **99** 5766.
 - [16] Granovetter M 1973 *Am. J. Sociol.* **78** 1360.
 - [17] Gleeson J P and Cahalane D J 2007 *Phys. Rev. E* **75** 056103.
 - [18] Singh P, Sreenivasan S, Szymanski B K and Korniss G 2013 *Sci. Rep.* **3** 2330.
 - [19] Dodds P S and Payne J L 2009 *Phys. Rev. E* **79** 066115.
 - [20] Whitney D E 2010 *Phys. Rev. E* **82** 066110.
 - [21] Gleeson J P 2008 *Phys. Rev. E* **77** 046117.
 - [22] Nematzadeh A, Ferrara E, Flammini A and Ahn Y Y 2014 *Phys. Rev. Lett.* **113** 088701.
 - [23] Brummitt C D, Lee K -M and Goh K-I 2012 *Phys. Rev. E* **85** 045102(R).
 - [24] Yağan O and Gligor V 2013 *Phys. Rev. E* **86** 036103.
 - [25] Dodds P S and Watts D J 2004. *Phys. Rev. Lett.* **92** 218701.
 - [26] Wang W, Tang M, Zhang H-F and Lai Y-C 2015 *Phys. Rev. E* **92** 012820.
 - [27] Zheng M, Lü L and Zhao M 2013 *Phys. Rev. E* **88** 012818.
 - [28] Centola D 2010 *Science* **329** 1194.
 - [29] Miller J C 2007 *Phys. Rev. E* **76** 010101.
 - [30] Yang H, Tang M and Gross T 2015 *Sci. Rep.* **5** 13122.
 - [31] Cui A-X, Wang W, Tang M, Fu Y, Liang X and Do Y 2014 *Chaos* **24** 033113.
 - [32] Jo H H, Perotti J I, Kaski K and Kertész J 2014 *Phys. Rev. X* **4** 011041.
 - [33] Wu C, Ji S, Zhang R, Chen L, Chen J, Li X and Hu Y 2014 *Europhys. Lett.* **107**, 48001.
 - [34] Hu Y, Ksherim B, Cohen R and Havlin S 2011 *Phys. Rev. E* **84**, 066116.
 - [35] Cellai D, Lawlor A, Dawson K A and Gleeson J P 2011 *Phys. Rev. Lett.* **107** 175703.
 - [36] Baxter G J, Dorogovtsev S N, Goltsev A V and Mendes J F F 2011 *Phys. Rev. E* **83** 051134.
 - [37] Lee K-M, Brummitt C D and Goh K-I 2014 *Phys. Rev. E* **90** 062816.
 - [38] Karsai M, Iñiguez G, Kaski K and Kertész J 2014 *J. R. Soc. Interface* **11** 101.
 - [39] Catanzaro M, Boguñá M and Pastor-Satorras R 2005 *Phys. Rev. E* **71** 027103.

- [40] Wang W, Shu P-P, Zhu Y-X, Tang M and Zhang Y-C 2015 *Chaos* **25** 103102.
- [41] Miller J C, Slim A C and Volz E M 2011 *J. R. Soc. Interface.* **10** 1098.
- [42] Miller J C and Volz E M 2013 *PLoS ONE* **8** e69162.
- [43] Wang W, Tang M, Zhang H-F, Gao H, Do Y and Liu Z-H 2014 *Phys. Rev. E* **90** 042803.
- [44] Karrer B and Newman M E J 2010 *Phys. Rev. E* **82** 016101.
- [45] Newman M E J, Strogatz S H and Watts D J 2001 *Phys. Rev. E* **64** 026118.
- [46] Strogatz S H 1994 *Nonlinear dynamics and chaos: with applications to physics, biology, chemistry and engineering* (Westview, Boulder, CO).
- [47] Dorogovtsev S N, Goltsev A V, and Mendes J F F 2008 *Rev. Mod. Phys.* **80** 1275.
- [48] Chen W, Schröder M, D'Souza M R 2014 *Phys. Rev. Lett.* **112** 155701.
- [49] Radicchi F 2015 *Phys. Rev. E* **91** 010801(R).
- [50] Ferreira S C, Castellano C and Pastor-Satorras R 2015 *Phys. Rev. E* **86** 041125.
- [51] Shu P, Wang W and Tang M 2015 *Chaos* **25** 063104.
- [52] Holme P, Kim B J, Yoon C N, and Han S K. 2002 *Phys. Rev. E* **65** 056109.